JOURNAL OF THE ROYAL SOCIETY Interface
FirstCite® e-publishing

J. R. Soc. Interface
doi:10.1098/rsif.2005.0037
Published online

Adherence to antiretroviral therapy and its impact on clinical outcome in HIV-infected patients

N. M. Ferguson[1,†,‡], C. A. Donnelly[1,‡], J. Hooper[1], A. C. Ghani[1], C. Fraser[1], L. M. Bartley[1], R. A. Rode[2], P. Vernazza[3], D. Lapins[4], S. L. Mayer[5] and R. M. Anderson[1]

[1]*Department of Infectious Disease Epidemiology, Faculty of Medicine, Imperial College London, Norfolk Place, London W2 1PG, UK*
[2]*Abbott Laboratories, 100 Abbott Park Road, Abbott Park, IL 60064-3500, USA*
[3]*Division of Infectious Diseases, Cantonal Hospital, St. Gallen 9007, Switzerland*
[4]*Clinical Partners Inc., PO Box 2006, Hyde Park, New York 12538, USA*
[5]*Pascal Group Inc., 27704 Silver Lake Road, Salem, WI 53168, USA*

We analyse data on patient adherence to prescribed regimens and surrogate markers of clinical outcome for 168 human immunodeficiency virus infected patients treated with antiretroviral therapy. Data on patient adherence consisted of dose-timing measurements collected for an average of 12 months per patient via electronic monitoring of bottle opening events. We first discuss how such data can be presented to highlight suboptimal adherence patterns and between-patient differences, before introducing two novel methods by which such data can be statistically modelled. Correlations between adherence and subsequent measures of viral load and $CD4^+$T-cell counts are then evaluated. We show that summary measures of short-term adherence, which incorporate pharmacokinetic and pharmacodynamic data on the monitored regimen, predict suboptimal trends in viral load and $CD4^+$T-cell counts better than measures based on adherence data alone.

Keywords: HIV; antiretroviral therapy; adherence; compliance; protease inhibitor; mathematical model

1. INTRODUCTION

The importance of good adherence to prescribed dose levels and dosing times on the clinical outcome of antiretroviral therapy has been clearly demonstrated by past studies (Vanhove *et al.* 1996; Frottier *et al.* 1998; Montaner *et al.* 1998; Bangsberg *et al.* 2000, 2001; Gross *et al.* 2001; Knobel *et al.* 2001; Masquelier *et al.* 2002; Alexander *et al.* 2003). The very high replication rate of human immunodeficiency virus (HIV) within the infected patient (Ho *et al.* 1995; Perelson *et al.* 1996, 1997; Ferguson *et al.* 1999) means that even single missed doses can permit substantial viral replication to resume, even if such replication might occur below the limits of detection for current assays. A particular concern with such replication is that it occurs on the background of suboptimal but still inhibitory concentrations of drug—imposing a significant selection pressure for outgrowth of resistant viral mutants.

However, the extent to which such concerns are likely to be realized for an individual patient depends not only on their adherence behaviour, but also on pharmacokinetic (PK) and pharmacodynamic (PD; namely, the action of the drug on the target organism—in this case, quantified by the degree of inhibition of viral replication) characteristics of the drugs comprising the patient's antiretroviral regimen (Ferguson 2002). Although the correlation between adherence behaviour and outcome has been well studied, a systematic examination of how that relationship is affected by drug properties is still lacking.

Here, we examine adherence data for a total of 168 patients from three cohorts where electronic monitoring of the timing of bottle opening events was undertaken. We first introduce methods to visualize dose timing, which provide deeper insight into adherence behaviour, before characterizing adherence patterns seen in these patients using a variety of summary measures of adherence. Visualizing patient adherence patterns gives insight into adherence behaviours, but simple and statistically robust summary measures are needed to gain a quantitative understanding of the variability of adherence within a patient population, and to correlate adherence with clinical outcome. These two goals are not necessarily synonymous. Capturing

[†]Author for correspondence (neil.ferguson@ic.ac.uk).
[‡]N.M.F. and C.A.D. contributed in equal part to this work.

Received 13 December 2004
Accepted 16 March 2005

adherence behaviour requires construction of a statistical model able to reproduce 'important' characteristics of observed patterns (Girard *et al.* 1998). Here, we introduce new approaches to the modelling of dose timings. The parameters of such models are themselves summary statistics which describe aspects of adherence behaviour. Their parameters can therefore be used to categorize different types of adherence patterns (or look at the social correlates of adherence) and thus potentially provide caregivers with tools aimed at improving patient adherence.

Conversely, in correlating adherence with clinical outcome, we would optimally like a single summary statistic that captures everything of clinical relevance in any pattern of adherence and is hence predictive of outcome. Towards this end, we use a simple mathematical model of viral replication and drug PK/PD to derive new statistics designed to predict the impact of observed patterns of adherence on viral load and $CD4^+$T-cell counts. We compare the performance of these statistics in predicting clinical outcome (in terms of viral load and $CD4^+$T-cell count) with that of simpler adherence statistics that do not incorporate PK or PD data.

2. PATIENT DATA

Data on the timings of pill bottle opening of the protease inhibitor (PI) component of antiretroviral therapeutic regimens were collected via electronic monitoring for a total of 168 patients for whom monitoring had taken place over a minimum of 90 days. Of these patients, 108 were treated in 1998 and 1999, and their data collated by Clinical Partners Inc., 23 patients were treated at the Kantonsspital St. Gallen, Switzerland, in 1998 and 1999 and 37 patients were treated in 2000 and 2001 as a part of trial M99-056. This trial was a phase I/II randomized, open-label, multi-centre study of lopinavir/ritonavir once daily (800/200 mg; investigational) versus twice daily (400/100 mg; approved) in combination with stavudine (d4T) and lamivudine (3TC) in HIV-infected antiretroviral-naive patients (Eron *et al.* 2004). A 90 day minimum monitoring period resulted in the exclusion of 12 patients from this analysis. A median of 12 months of adherence data was available for each patient. Data on prescribed regimens together with viral load and $CD4^+$T-cell count measurements (taken on average every three months) were also available for all patients. For the 131 patients from the Clinical Partners Inc. and St. Gallen cohorts, the lower limit of quantification (LOQ) for viral load measurements was 400 copies ml^{-1}, while for the 37 patients in trial M99-056 the LOQ was 50 copies ml^{-1}. We therefore used greater than 400 copies ml^{-1} as the threshold for virological rebound in the analyses presented here.

The most common PIs recorded in the study population were saquinavir, indinavir and ritonavir (RTV). This reflects the period over which most of the data were collected. Substantial numbers of patients using dual PI or ritonavir boosted regimens participated in the Clinical Partners Inc. cohort, while lopinavir/ritonavir use was solely represented by trial M99-056. Table 1 gives summary details of the range of prescribed PI regimens represented in the combined dataset. The range of 'off-label' dosing levels and frequencies seen in table 1 should be noted.

Electronic monitoring of pill bottle opening events provides much more detailed information on adherence patterns than cruder quantitative measures (e.g. pill counts), and is arguably more objective than self-reported assessments of adherence (Kastrissios *et al.* 1998; Melbourne *et al.* 1999; Miller & Hays 2000; McNabb *et al.* 2003). That said, the timing of bottle opening events is not a perfect measure; patients may remove more than the prescribed dose from a bottle during a single opening (e.g. to avoid taking the bottle with them all day), or may open a bottle without removing any pills. However, correlating pill counts with electronic monitoring data can detect such issues in many cases.

3. VISUALIZING ADHERENCE DATA

The raw data for each patient were formatted as a list of sequential dates and times corresponding to the opening of the medication container, denoted by $\boldsymbol{x} = (x_1, x_2, \ldots, x_{\mathrm{ND}})$, where x_{ND} corresponds to the last recorded opening. An example of the data collected is shown in the first column of figure 1, where the date (day) and corresponding time of the pill bottle openings are plotted in an x–y scatter-plot. It can be seen from these graphs that in general individuals endeavour to take their pills at the same time each day.

A common representation of adherence data is in terms of adherence to the prescribed number of daily doses. This provides an initial impression of an individual's average or long-term adherence behaviour with respect to pill counts. The empirical distribution of the number of days on which n pills are taken ($n=0, 1, \ldots, N$) is shown in the second column of figure 1.

By simply presenting the data in these two ways, two key and quite distinct aspects of adherence behaviour have been highlighted—adherence to the prescribed number of daily doses and adherence to a nominal dose time. A thorough summary of adherence behaviour should capture both of these aspects, given that good adherence to the prescribed number of daily doses does not necessarily imply high levels of adherence to a nominal dose time.

Because patients with the same dose-frequency adherence can have very different dose-timing patterns, a more detailed measure that quantifies this variation in behaviour is required. Adherence to the prescribed dosing interval is an obvious measure that can be used to assess the level of patient adherence to a prescribed regimen, because the interval between adjacent doses should determine trough drug concentration in plasma and thus the adequacy of inhibition of viral replication.

The third column of figure 1 shows how representing dose-timing data by a plot of one dose interval, $\delta_i = x_{i+1} - x_i$ against the next can provide valuable information about adherence behaviour not apparent from the earlier representations. Perfect dose-timing and dose-frequency adherence is represented as a single point at the prescribed dosing interval T. Poor

Table 1. Numbers of patients prescribed the different protease inhibitor (PI) regimens represented in the combined dataset. (The terms QD, BID and TID refer to a prescribed dosing frequency of one, two or three doses per day, respectively. Lopinavir is listed as a single PI below, though is always prescribed with co-formulated low dose ritonavir.)

			number of patients prescribed regimen					
dosing frequency	drug	dose (mg)	taken as sole PI	taken with indinavir	taken with lopinavir	taken with nelfinavir	taken with ritonavir	taken with saquinavir
QD	lopinavir	800	18		—			
	nelfinavir	1250	1			—		
BID	indinavir	400	3	—			1	
		800	2	—				
		1000	1	—				
		1200	15	—		1		3
	lopinavir	400	35		—			
	nelfinavir	500	1			—		
		750	2			—		
		1250	12	1		—		1
	ritonavir	100	3				—	3
		200	3				—	3
		300	2	1			—	
		400	23				—	20
		500	2				—	2
		600	9				—	4
	saquinavir[a]	200	2				2	—
		400	15	2			9	—
		600	20	1			18	—
		800	2				1	—
		1000	1					—
		1200	4			1	2	—
TID	indinavir	400	1	—				
		800	36	—		1		
		1000	1	—				
		1200	4	—				
	nelfinavir	250	1			—		
		600	1			—		
		750	15	1		—		2
		1000	2			—		1
	saquinavir	600	8			1		—
		800	1			1		—
		1200	3			1		—

[a] Soft gel (Fortovase) formulation of saquinavir.

dose-timing adherence is represented by scatter about the point (T, T), while poor dose-frequency adherence is represented by the occurrence of points at dose intervals which are a multiple of T. A common feature of such plots is serial dependence between adjacent dose intervals, indicated by a tendency of points to lie on the $x+y=2T$ diagonal line. This reflects a systematic bias away from equal adjacent dose intervals; for example, someone on a BID regimen who took drug at 08.00 and 23.00 each day would generate a plot with 2 points at (9, 15) and (15, 9).

A variant on the interval–interval plot is given by plotting the time of day of one dose against the time-interval between doses (fourth column, figure 1). This again has the advantage of clearly representing both dose-timing and dose-frequency adherence—the former by the degree of scatter about the prescribed dosing times on the x-axis, and the latter by the proportion of points seen at $2T$ or above on the y-axis.

Lastly, another form of suboptimal adherence, which is not well represented by plots intended to highlight dose-frequency or dose-timing adherence, is the failure to take many doses in succession—so-called 'drug holidays'. These are typically multi-day (e.g. weekend or longer) periods during which drug is not taken, and are best visualized using plots of the type shown in the first column of figure 1. Such a drug holiday is clearly evident in patient shown in figure 1*d*.

4. MODELLING ADHERENCE BEHAVIOUR

Currently, adherence is usually described by indices which only summarize dose-frequency adherence, the most commonly used being the fraction of doses taken, p, and the daily count adherence (fraction of days the prescribed number of doses are taken), c. This is largely because detailed dose-timing information was rarely available until the advent of electronic monitoring.

Even with such limited summary information, a simple Markov model of dosing behaviour can be constructed (Girard *et al.* 1998; Wong *et al.* 2003), in which p represents the probability that the next dose will be taken. Equivalently, if there are N doses prescribed

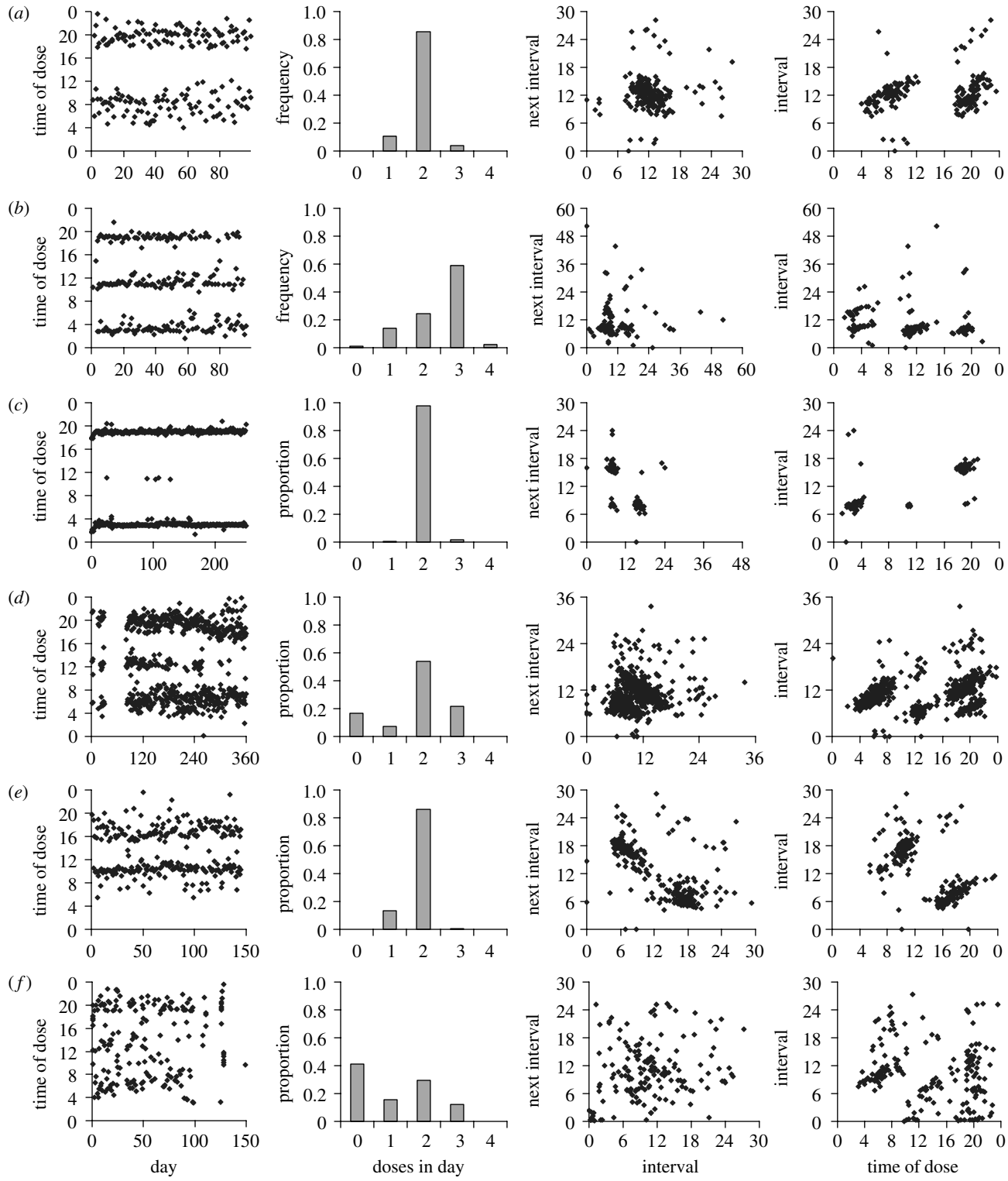

Figure 1. Adherence data for a representative sample of patients (*a*) N126 (BID regimen), (*b*) H013 (TID), (*c*) 2203 (BID), (*d*) H021 (TID), (*e*) L109 (BID) and (*f*) H011 (BID). First column: times of doses of drug against day of monitoring. Second column: frequency distribution for number of pills taken per day. Third column: plots of dose interval (time between two consecutive doses) against the next dose interval. Fourth column: scatter plots of time of dose against the interval from the previous dose. For all plots, a day is defined as 03.00 to 03.00 the next day, so time 00.00 in real time represents 03.00 on the graphs.

per day, then this model equates to assuming the number of doses taken in time period T is binomially distributed as $\mathrm{Bin}(p, NT)$ with mean pNT and variance $p(1-p)NT$. As seen in figure 2, this simple dosing model fits patterns of frequency adherence very well for many patients, so long as overall adherence levels are stationary through time and drug holidays are excluded from the data.

Elaborations of this approach involve moving from a 1-stage Markov model to a two- or three-stage model in which the probability of the next dose being taken is

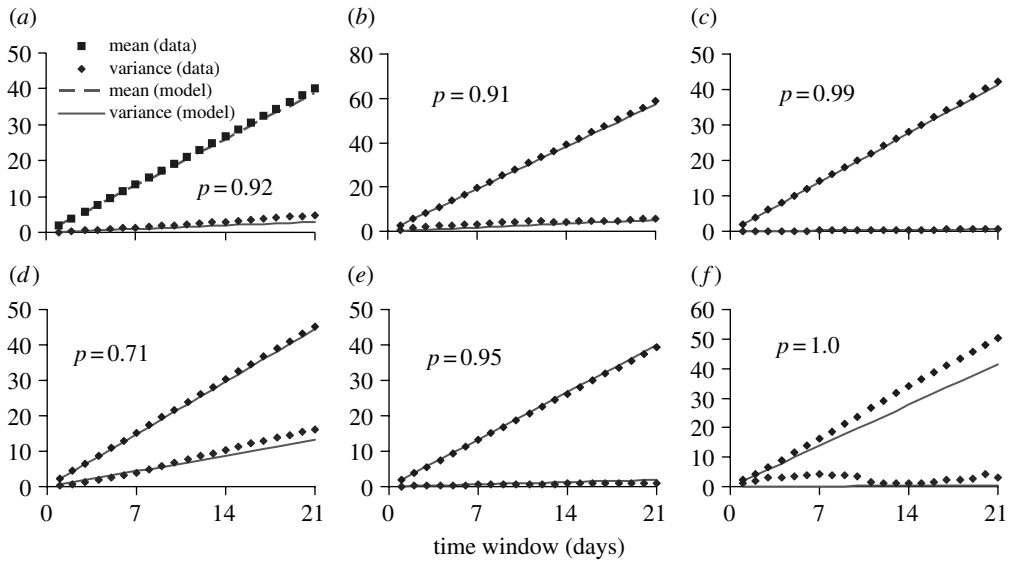

Figure 2. Variance and mean of the number of doses taken in a time window (y-axis) plotted against duration of that window, T(x-axis). For each patient, the variance is calculated across all windows of duration T that do not include a drug holiday (defined to be a period of 2 or more days without a dose being taken). For (a)–(f), results are for the same patients as in figure 1. For (b) and (f), only the first 10 weeks of the data shown in figure 1 were used, while for (d), data from weeks 16–26 were used. This was a result of significant temporal changes in overall adherence levels outside these periods.

conditional on whether the previous one or two doses were taken (Girard *et al.* 1998).

However, all such models solely describe dose-frequency adherence. To incorporate dose-timing adherence into the model, a number of approaches are possible. One of the more sophisticated approaches is to fit (using maximum-likelihood methods) a flexible parametric or smoother non-parametric bivariate multimodal probability density function to empirical joint distributions of dose times and inter-dosing intervals. An example of the results of fitting sophisticated multivariate models of dose timing to empirical joint distributions of dose times and inter-dosing intervals (Hooper 2002) is shown in figure 3. Such models can be used to simulate adherence behaviour which in turn could be used in the PD modelling of drug action, or the mathematical modelling of within-patient viral dynamics (Ferguson 2002). They can capture much of the detail of observed adherence behaviour (including time-of-day biases, compensatory behaviour and conditionality of the type included in the two-stage Markov model). The drawback of such models is that they are mathematically complex and the parameter estimates generated from the models are difficult to interpret. As such, while these types of approaches may represent the gold standard of future adherence modelling, there is a more immediate need for simpler, more intuitive models. Therefore, we focus here on simpler approaches that build incrementally on past work.

We assume a binomial model Bin(p, N) for the number of doses in a day (justified by the fit of the binomial model to long-term variance–time curves; see figure 2). The boundary of a day is best selected to be a time of minimum dosing frequency, such as 03.00, rather than midnight, given a significant fraction of individuals take their 'evening' dose for a day after midnight, before sleeping. Each 24 h period is then divided into N equal width $24/N$ hour sequential

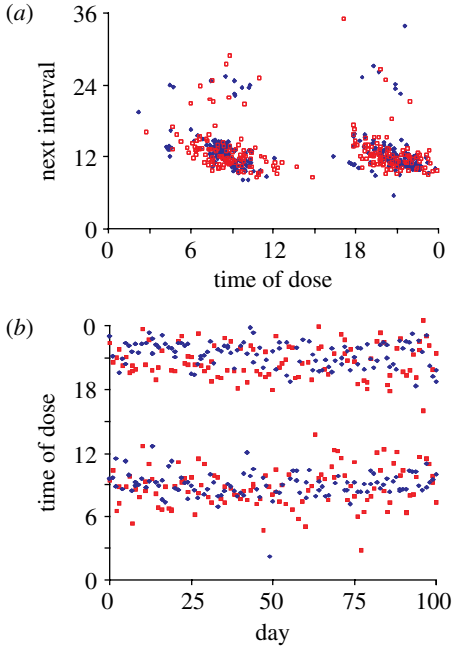

Figure 3. Maximum-likelihood fit of a bivariate lognormal mixture model of the joint distribution of time of dose and inter-dose interval (as shown in fourth column of figure 1). Blue points represent data for patient L097 (on a BID regimen), and red points represent simulated data generated from the best-fit parameter set. (a) Dose time against next dose interval. (b) Day of observation against time of dose, showing how the model accurately captures patterns of adherence behaviour.

windows, labelled j=1, 2, …, N. The distribution of dose times in the jth dosing window is then modelled as a truncated normal density function

$$p(t_j = t) = \frac{f(t|\tau_j, \sigma_j)}{\int_{t_{S,j}}^{t_{S,j}+24/N} f(t|\tau_j, \sigma_j)\mathrm{d}t},$$

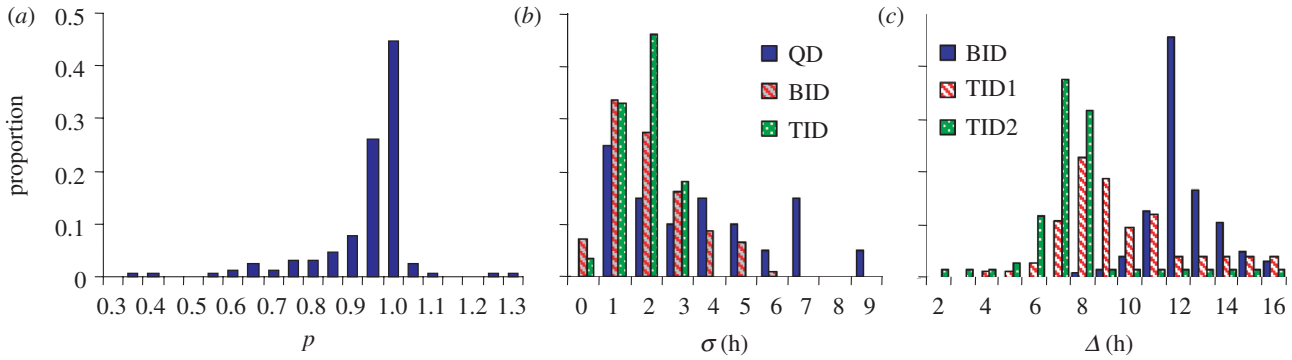

Figure 4. Distributions of the estimates of (*a*) p, (*b*) σ and (*c*) Δ_j using data from all 168 patients for the binomial dosing model with truncated normal-distributed dose timing (see main text). In (*b*), estimates of σ are shown stratified by prescribed frequency of dosing. Dose-timing error, σ, is significantly larger for patients receiving QD regimens compared with patients receiving BID or TID regimens. In (*c*), the Δ_j are estimated as the mean inter-dose interval between the first and second doses taken in a day for BID regimens, and between the first and second (TID1) and the second and third (TID2) for TID regimens.

where

$$f(t|\tau_j, \sigma_j) = \exp\left(-\frac{1}{2}\left(\frac{t-\tau_j}{\sigma_j}\right)^2\right).$$

Here, $t_{S,j}$ is the start time of the jth window, τ_j is the mode of the time distribution of the jth daily dose and σ_j characterizes the timing error of the jth dose. So long as $\sigma_j \ll \tau_j - t_{S,j}$ and $\sigma_j \ll t_{S,j} + 24/N - \tau_j$ (assuming time units of hours), as is mostly the case, τ_j is approximately equal to the average time at which the jth dose is taken. Hence, the mean and standard deviation of the dose times in the jth window are usually a good approximation to the maximum-likelihood estimates of τ_j and σ_j.

In general, we found no clear difference between the dosing errors for different dosing intervals j for the patient data we examined. Hence, the above model can be simplified by assuming $\sigma_j = \sigma$ for all j. Additionally, one of the τ_j is uninformative (therapeutic benefit is determined only by the interval between doses, not by the time of day of the first dose). Hence, we are left with a model with $N+1$ informative parameters—p, σ and $\Delta_j = \tau_{j+1} - \tau_j$, where $j = 1, 2, \ldots, N-1$. All are intuitively interpretable—p is the proportion of doses taken, σ is the standard deviation of the random dose-timing error and Δ_j represents any systematic dose-timing bias.

Because systematic biases in dosing periods observed for a few patients tend to be related to the habitual missing of particular doses each day, the model can usefully be generalized to model the probability of taking a dose in each dosing window separately, using a Bernoulli distribution with dosing window-specific mean p_j. In addition, some patients exhibit correlations between the timing errors of adjacent doses. However, such effects are relatively minor (Hooper 2002).

Fitting the latter model to the dose-timing data for all 168 patients, figure 4 shows the resulting distributions of the estimated values for p, σ and Δ_j, while figure 5 shows the joint distribution of estimates of p and σ. As perhaps might be expected, very good dose-timing adherence ($\sigma < ca$ 0.5 h) is highly predictive of excellent dose-frequency adherence, but the converse was not true.

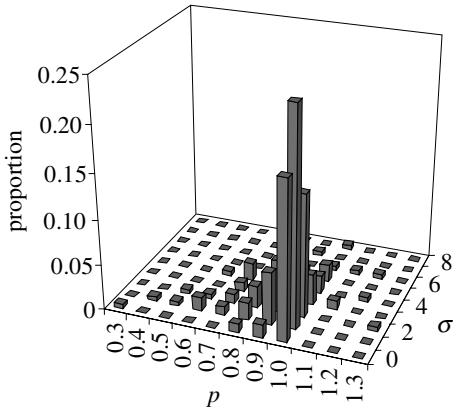

Figure 5. Joint distribution of the estimates of p and σ using data from all 168 patients. Many more patients are dose-frequency adherent than are timing adherent.

Small mean differences were observed in the values of p for subjects enrolled in the Clinical Partners (0.91 ± 0.02), St. Gallen (0.96 ± 0.05) and M99-056 (0.98 ± 0.03) cohorts. In addition, no significant difference was seen in the estimated values of Δ_j. Significant differences were noted, however, in timing adherence between subjects enrolled in the Clinical Partners Inc. cohort and the other two cohorts. For instance, for BID regimens, $\sigma = 2.5 \pm 0.3$ for subjects in the Clinical Partners Inc. cohort, $\sigma = 1.5 \pm 0.5$ for subjects in the St. Gallen cohort and $\sigma = 1.6 \pm 0.4$ for subjects in the M99-056 cohort.

This model does not attempt to capture another form of non-adherence—long periods of time during which drug is not taken, often termed drug holidays. Figure 6 shows the distribution of the number of drug holidays taken across the patient population and the duration of these holidays. A drug holiday is defined here as a period of two or more days during which no drug is taken.

A number of patients show discontinuous changes in adherence behaviour at certain times—perhaps associated with regimen or lifestyle changes. For example, in the combined dataset examined, 39 patients experienced at least one regimen change involving a change in dose frequency. Models of the type discussed above are

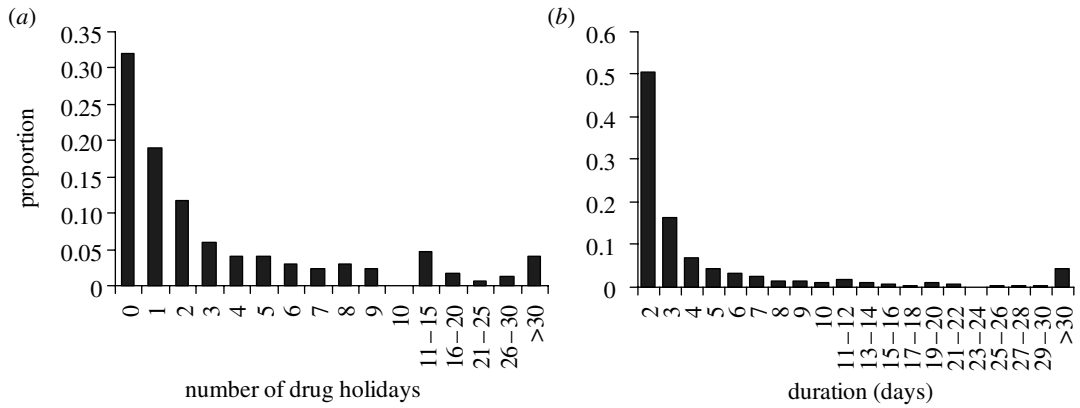

Figure 6. (*a*) Distribution (across all 168 patients) of the number of drug holidays (periods of 2 days or more where no doses were taken) observed per patient. (*b*) Distribution of the duration of drug holidays across all 168 patients (2 days being, by definition, the minimum duration).

only suitable for modelling relatively stationary adherence time-series. Therefore, where discontinuous changes occur, the model must be fitted separately to the data collected in the time periods between such discontinuities.

A certain degree of arbitrariness remains in the definition of the model—for instance in the assignment of the start times of the N dosing periods, $t_{S,j}$. The choice used here (i.e. starting the day at 03.00) attempts to minimize the chance of incorrect classification of individual doses into the wrong dosing interval, but such boundary effects are impossible to eliminate completely. Some improvement might be possible by defining the dosing periods to be symmetrical about the τ_j, and only estimating the τ_j from days where all N doses are taken, but we did not investigate the (probably limited) benefits to be obtained, through such an increase in model complexity. Lastly, the model does not allow for over-dosing. The frequency of over-dosing within a day was low—32 patients showed some evidence of overdosing for one or more elements of their regimen, but the level of excess dosing was low, with only seven patients taking more than 105% of the prescribed number of doses. Furthermore, the relationship between inhibition and concentration for simple $E_{\max}$ models appropriate for characterizing antiretroviral agents (Ferguson *et al.* 2001) indicates the effect of an excess dose on virological suppression is minor compared with the impact of missing a dose (provided that the patient did not experience a safety/tolerability-related event that could have affected plasma drug levels associated with the antiretroviral regimen being used).

5. DERIVATION OF CLINICALLY PREDICTIVE SUMMARY MEASURES OF ADHERENCE

The negative impact of poor adherence on clinical outcome (as quantified using surrogate markers of clinical outcome such as plasma viral load or $CD4^+$ T-cell count) has been demonstrated with a wide range of summary measures of adherence behaviour, including some of the statistics discussed above (Vanhove *et al.* 1996; Frottier *et al.* 1998; Montaner *et al.* 1998; Bangsberg *et al.* 2000, 2001; Gross *et al.* 2001; Knobel *et al.* 2001; Masquelier *et al.* 2002; Alexander *et al.* 2003). This past work allows the construction of statistical models to predict the probable impact of any particular pattern of adherence on outcome. However, such models are purely correlative rather than mechanistic—that is, they do not attempt to estimate the impact of irregular dosing on drug effectiveness and thus the probable impact on viral replication.

Here, we construct a simple mathematical model that translates dosing times collected via electronic monitoring into drug concentrations through time. The model then estimates the impact of those varying drug levels on suppression of viral replication and thus the extent of residual viral replication likely to occur during any monitored period of therapy. The model developed is very simple and ignores PK and PD variability between patients, variation in drug concentrations in different body tissues, evolution of resistant virus (though the model output can be seen as predictive of when resistance might be expected to evolve) and details of the interaction between HIV and its target cell population (see Wahl & Nowak (2000) for a more detailed treatment of HIV and T-cell dynamics in the context of adherence modelling). Our aim was to create pharmacologically motivated statistics summarizing adherence behaviour and to explore whether these were better predictors of clinical outcome than the simple dose-frequency and dose-timing adherence statistics discussed earlier.

The first stage—generating predicted concentrations of drug through time from dosing time-series—is, in principle, straightforward, requiring only a suitably validated multiple dosing PK model for each drug in use. However, in practice, drug interactions, nonlinear clearance, protein binding and induction processes make detailed modelling complex. We therefore adopt the simplest possible PK model—zero-order absorption, first-order clearance, with no drug interactions

$$C^{\mathrm{A}}(t) = \sum_{i:x_i<t} C^{\mathrm{A}}_{\max} 2^{-(t-x_i^{\mathrm{A}})/\kappa^{\mathrm{A}}} \approx C^{\mathrm{A}}_{\max} 2^{-(t-x^{\mathrm{A}}_{\mathrm{last}})/\kappa^{\mathrm{A}}}.$$

Table 2. Pharmacokinetic/pharmacodynamic (PK/PD) parameters for licensed protease inhibitors, as derived from the literature.

(κ is the effective half-life of drug—i.e. the half-life allowing for induction effects; $C_{\max}$ is the peak concentration of drug reached after taking a dose; protein-bound and non-bound.)

drug	regimen	dose (mg)	κ (h)	$C_{\max}$ (μg ml^{-1})	IC_{50}[a] (μg ml^{-1})	references
amprenavir	BID	1200	2.6[b] (2–10; 4.8[b] with RTV)	7.7 (3–8)	0.28$\pm$0.2	Adkins & Faulds (1998) and GlaxoSmithKline (2002)
indinavir	TID	800	1.4[b] (1–2; 3.2 with RTV 100)	7.7 (5–11; 50% greater with RTV)	0.06$\pm$0.02	Merck & Co., Inc. (1999) and van Heeswijk *et al.* (1999)
nelfinavir	BID	1250	5.4$\pm$2, 7.1$\pm$2.5 with RTV	3.6$\pm$0.8, 4.3$\pm$1 with RTV	0.52$\pm$0.3	Jarvis & Faulds (1998) and Kurowski *et al.* (2002)
ritonavir	BID	600	3.2 (3–5)	11.2$\pm$3.6	0.96$\pm$0.2	Abbott (1999)
saquinavir[c]	BID	800	3.2[b] (4.9–8.7) with RTV (Buss *et al.* 2001)	0.53 (0.2–4), 4.5 (2.8–7.3) with RTV (Buss *et al.* 2001)	0.25$\pm$0.2	Barry *et al.* (1997) and Roche (1997)
lopinavir/ ritonavir	BID	400	5–6	9.0 (7–11)	0.06$\pm$0.03	Abbott (2001)

[a] Values are averages of values measured in 50% human serum to HIV wild-type laboratory strains IIIB, pNL4-3 and HXB2 (Molla *et al.* 1998).
[b] These half-lives are calculated to be consistent with $C_{\min}$ and area under curve (AUC) measurements under the assumption of instantaneous absorption and first-order elimination. This was because for many studies the quoted direct estimates of plasma concentration decay slopes averaged across patients are inconsistent with quoted $C_{\min}$ and AUC values assuming the simplified PK model used here.
[c] The values quoted apply to Fortovase. Invirase is assumed to have the same IC_{50} and κ values, but 50% of the $C_{\max}$ of the same dose of Fortovase.

Here, $C^{\mathrm{A}}(t)$ is the concentration of drug A at time t, $C^{\mathrm{A}}_{\max}$ is the peak concentration of drug reached after taking a dose, x^{A}_i is the chronological time that dose i of drug A was taken and κ^{A} is the 'effective half-life' of drug; that is, the half-life allowing for induction effects (i.e. from low dose ritonavir used as a PK enhancer; see §7 below). The approximate equality (where $x^{\mathrm{A}}_{\mathrm{last}}$ is the time of the last dose before time t) holds if κ^{A} is much smaller than any likely inter-dose interval (i.e. $2^{-\Delta/\kappa^{\mathrm{A}}} \ll 1$). Table 2 lists the PK and PD parameter values assumed for the PIs used by the patients included in this analysis. We assume that within the dose ranges observed, $C^{\mathrm{A}}_{\max}$ scales linearly with dose.

We then need to translate drug concentration into PD effect; namely, the extent to which drug inhibits viral replication. We assume a simple $E_{\max}$ model with a slope parameter of unity (Ferguson *et al.* 2001)

$$I(t) = 1 - \frac{1}{C^{\mathrm{A}}(t)/\mathrm{IC}^{\mathrm{A}}_{50} + 1},$$

where $\mathrm{IC}^{\mathrm{A}}_{50}$ is the concentration of drug A at which 50% inhibition is achieved. There are multiple issues surrounding the measurement of IC_{50} and PD response more generally (Ferguson *et al.* 2001), but one of the most important factors for PIs is to correctly account for protein binding. Therefore, we use IC_{50} values measured in the presence of human serum (Molla *et al.* 1998).

The above formulation accounts for inhibition due to a single drug only. In the case of multiple drugs acting non-synergistically (Ferguson *et al.* 2001), the combined effect of two drugs, A and B, from the same class is additive,

$$I(t) = 1 - \frac{1}{C^{\mathrm{A}}(t)/\mathrm{IC}^{\mathrm{A}}_{50} + C^{\mathrm{B}}(t)/\mathrm{IC}^{\mathrm{B}}_{50} + 1},$$

while the combined effect of two drugs, A and C, from different classes is multiplicative,

$$I(t) = 1 - \frac{1}{(C^{\mathrm{A}}(t)/\mathrm{IC}^{\mathrm{A}}_{50} + 1)(C^{\mathrm{C}}(t)/\mathrm{IC}^{\mathrm{C}}_{50} + 1)}.$$

However, for this study, only dose-timing data on the PI component of regimens were available for all patients. Hence, we model inhibition from that component of the regimen only. Furthermore, while 40% of patients studied were at some point on a multiple PI regimen (excluding those on lopinavir/ritonavir), in 51% of these, this regimen consisted of ritonavir plus another PI. For such regimens the effect of ritonavir in inhibiting the cytochrome P-450 CYP3A metabolism of other PIs outweighs the viral inhibitory effect of ritonavir itself (Kempf *et al.* 1997; Hsu *et al.* 1998). Hence, for simplicity, we assume such dual PI therapy can be modelled as a single drug, but use PK parameters for the non-ritonavir PI adjusted for the PK-enhancing effect of ritonavir (see table 2). Furthermore, we do not distinguish between different dose levels of ritonavir; a patient is classified as being on a PK-enhanced PI regimen on a particular day if they took one or more doses of ritonavir that day, plus one or more doses of another PI. These assumptions clearly represent an approximation given ritonavir may have an antiretroviral effect at doses as low as 200 mg BID. However,

these effects are likely to be small by comparison to the antiretroviral action of the 'boosted' PI.

The final and most tentative step is using estimated inhibition time-series to evaluate the probable impact of drug on virus replication. A wide variety of complex models are possible, but most cannot be solved analytically, limiting their usefulness as a simple transform of adherence data. We therefore adopt a simple exponential growth model. This is then modified heuristically to impose maximum and minimum limits on viral load, so as to mimic the effect of the long-lived infected ($CD4^+$T-cell or macrophage) cell pool in sustaining virus (Perelson *et al.* 1997; Ferguson *et al.* 1999) even under effective therapy, and target-cell saturation or immune-limited viral replication when drug is ineffective (De Boer & Perelson 1998; Fraser *et al.* 2001). Our model of exponential growth is

$$\frac{\mathrm{d}V}{\mathrm{d}t} = r[1 - I(t)]\,V - \alpha\,V,$$

where r is the replication rate of virus in the absence of drug, and α is the decay rate of virus when inhibition is complete. The former parameter is best estimated from the rebound kinetics of viral load seen in patients undergoing treatment interruption (Frost *et al.* 2002), although data from primary infection can also be useful (Little *et al.* 1999). Available data indicate $r = 1/12\ \mathrm{h}^{-1}$ (i.e. $2\ \mathrm{d}^{-1}$) to be reasonable. The latter parameter is determined not by the half-life of virions in plasma, but by the slower time-scale process of infected activated $CD4^+$T-cell death (Ho *et al.* 1995; Perelson *et al.* 1996, 1997; Ferguson *et al.* 1999). A value of $\alpha = 1/24\ \mathrm{h}^{-1}$ (i.e. $1\ \mathrm{d}^{-1}$) is assumed here.

The solution of this equation is

$$\Omega_i = \frac{V_{i+1}}{V_i} = \exp\left[r\int_{x_i}^{x_{i+1}}[1 - I(t)]\mathrm{d}t - \alpha(x_{i+1} - x_i)\right],$$

where V_{i+1} and V_i are the viral loads at the time the $(i+1)$th and ith monitored drug dose were taken respectively, and Ω_i is their ratio.

Substituting in for $I(t)$ for a single drug and evaluating the integral gives, with some manipulation,

$$\Omega_i = \left(\frac{C^{\mathrm{A}}_{\max}/\mathrm{IC}^{\mathrm{A}}_{50} + 2^{\delta_i/\kappa}}{C^{\mathrm{A}}_{\max}/\mathrm{IC}^{\mathrm{A}}_{50} + 1}\right)^{\kappa r/\ln 2} \exp[-\alpha\delta_i],$$

where $\delta_i = x_{i+1} - x_i$.

The expected viral load at dose time i can then be calculated as

$$V_i = V_0\prod_{j=0}^{i-1}\Omega_j. \tag{5.1}$$

In this context, our approach of modelling multiple PIs as a single boosted PI has the advantage that inhibition can be calculated as if generated by a single drug. In this case, the simpler mathematical formulation means that the above closed-form solution for expected viral replication can be used. If multiple drugs were explicitly modelled, then the more complex expression for inhibition would necessitate numerical evaluation of the integral over inhibition between doses. This would complicate the analysis substantially.

As it stands, this model predicts that viral load can fall at the first phase exponential decay rate (Ho *et al.* 1995; Perelson *et al.* 1997) without limit, or conversely can grow without limit if drug-induced inhibition of replication is inadequate. We therefore employ a simple heuristic mechanism for limiting maximum and minimum viral load. If V_i is the estimated viral load at dose time i, then V_{i+1} is given by

$$V_{i+1} = V_{\min} + (V_{\max} - V_{\min})\tanh\left[\frac{V_i - V_{\min}}{V_{\max} - V_{\min}} \times \left(\frac{C^{\mathrm{A}}_{\max}/\mathrm{IC}^{\mathrm{A}}_{50} + 2^{\delta_i/\kappa}}{C^{\mathrm{A}}_{\max}/\mathrm{IC}^{\mathrm{A}}_{50} + 1}\right)^{\kappa r/\ln 2} \exp[-\alpha\delta_i]\right], \tag{5.2}$$

where $V_{\min}$ is the minimum viral load, and $V_{\max}$ is the maximum attainable set point viral load (here assumed to be 10^6 copies ml^{-1}). The precise value of $V_{\min}$ is uncertain, but since a low residual level of viral replication is known to occur under even the most potent regimens (Ferguson *et al.* 1999; Fraser *et al.* 2001), we assume a value of 1 copy ml^{-1}; below the limits of quantification of currently available commercial assays. Equation (5.2) is iterated to calculate V_i from V_0. As $V_{\max} \to \infty$ and for $V_{\min} = 0$, this model reduces to the earlier non-limited form. It should be noted that while a $\tanh(x)$ functional form is used in equation (5.2), other saturating functions, which are linear for small values of the argument, could equally be used.

Subsequent development of this model to link the adherence patterns and PK/PD properties to $CD4^+$T-cell counts would require additional assumptions and simplifications. Furthermore, given the relative simplicity of this model and the many patient-specific factors it ignores, we do not expect to be precisely predictive of viral load at a given time point. Thus, we test how these measures are correlated with viral load and $CD4^+$T-cell measurements for our patient data.

6. CORRELATION OF ADHERENCE WITH OUTCOME

In examining the correlation between adherence and outcome, a number of approaches are possible. Much previous work (Vanhove *et al.* 1996; Frottier *et al.* 1998; Montaner *et al.* 1998; Bangsberg *et al.* 2000, 2001; Gross *et al.* 2001; Knobel *et al.* 2001; Masquelier *et al.* 2002; Alexander *et al.* 2003) has compared aggregate outcome measures (e.g. proportion of viral load measures below detectable, viral load at a certain time point, or $CD4^+$T-cell increase since start of therapy) with similar long-term average measures of adherence to establish the broad importance of adherence to successful therapeutic outcome.

Here, we use a different approach, and instead examine the correlation between individual viral load and $CD4^+$T-cell count measurements through time with adherence in a period of time leading up to those measurements being taken. In undertaking such an analysis, it is of particular interest to determine the time

Table 3. Correlation in adherence measures (calculated over the 7 days before clinical measurements, except L_2) overall (with p-value, given below the diagonal, obtained assuming all observations are independent) and patient-specific (median and interquartile range given above the diagonal).

(pIC_{50}, L_1 and L_2 incorporate pharmacokinetic/pharmacodynamic (PK/PD) properties of the drugs.)

	p	s.d.	var	pIC_{50}	L_1	L_2
p	1	−0.612 (−0.955, 0.233)	−0.585 (−0.953, 0.201)	−0.803 (−0.989, −0.432)	−0.836 (−0.976, −0.370)	−0.48 (−0.830, −0.025)
s.d.	−0.574 ($p<0.0001$)	1	0.997 (0.985, 1.000)	0.945 (0.821, 0.999)	0.945 (0.634, 0.992)	0.426 (−0.201, 0.884)
var	−0.458 ($p<0.0001$)	0.865 ($p<0.0001$)	1	0.977 (0.854, 1.000)	0.956 (0.624, 0.997)	0.446 (−0.173, 0.890)
pIC_{50}	−0.397 ($p<0.0001$)	0.523 ($p<0.0001$)	0.432 ($p<0.0001$)	1	0.996 (0.963, 1.000)	0.547 (0.087, 0.962)
L_1	−0.264 ($p<0.0001$)	0.38 ($p<0.0001$)	0.311 ($p<0.0001$)	0.85 ($p<0.0001$)	1	0.483 (−0.074, 0.832)
L_2	−0.328 ($p<0.0001$)	0.339 ($p<0.0001$)	0.191 ($p<0.0001$)	0.562 ($p<0.0001$)	0.663 ($p<0.0001$)	1

period prior to outcome measurement for which different adherence measures are most predictive. The multiple time-scales involved in HIV pathogenesis (Ferguson *et al.* 1999; Fraser *et al.* 2001) mean that making *a priori* estimates of this time period is difficult. In the absence of drugs, viral load typically rebounds to above detectable levels in a matter of days to weeks (Frost *et al.* 2002), so it might be expected this would also be the most relevant time-scale when correlating adherence with viral load measures. However, long-term suppression depends on consistently good adherence, so adherence measured over longer time-scales might also be expected to be predictive. $CD4^+$ T-cell counts have dynamics occurring on a somewhat slower time-scale. Therefore, it might be expected that this outcome measure is less sensitive to short-term adherence patterns, and more dependent on longer-term behaviour.

We focus on two binary outcome measures (viral load ≤ 400 copies ml^{-1} and $CD4^+$ T-cell count ≤ 600 cells mm^{-3}) and test their associations, using logistic regression, with measures of both dose-timing and dose-frequency adherence. Specifically, these measures are the proportion of doses taken, variance and standard deviatian of inter-dose interval, the estimated proportion of time with drug concentration below IC_{50}, denoted pIC_{50}, as well as the two measures of residual viral replication. The viral load threshold was chosen to be 400 copies ml^{-1} because this was the threshold for detection for the Clinical Partners Inc. and St. Gallen patients. The value of 600 cells mm^{-3} chosen for $CD4^+$ T-cell count threshold is a relatively demanding measure of clinical success, but sensitivity analysis varying this threshold showed that, for the patient population studied, this choice gave the binary $CD4^+$ T-cell count outcome which was best predicted by the adherence measures examined. These viral-replication-related measures were defined to be the log of predicted viral load as previously derived (see equations (5.1) and (5.2) above) such that

$$L_1 = \log\left(V_0 \prod_{j=0}^{i-1} \Omega_j\right) = \log(V_0) + \sum_{j=0}^{i-1} \log(\Omega_j),$$

and ignoring the additive constant

$$L_1 = \sum_{j=0}^{i-1} \log(\Omega_j).$$

$$L_2 = \log\left(V_{\min} + (V_{\max} - V_{\min})\tanh\left[\frac{V_i - V_{\min}}{V_{\max} - V_{\min}} \times \left(\frac{C^{\mathrm{A}}_{\max}/\mathrm{IC}^{\mathrm{A}}_{50} + 2^{\delta_i/\kappa}}{C^{\mathrm{A}}_{\max}/\mathrm{IC}^{\mathrm{A}}_{50} + 1}\right)^{\kappa r/\ln 2} \exp[-\alpha\delta_i]\right]\right).$$

The predictors, except for L_2, were calculated over various time-intervals (3, 5, 7, 14, 21, 28 and 35 days) prior to the clinical measurement.

Analyses were undertaken using both simple logistic regression and generalized estimating equations (GEE; Liang & Zeger 1986; Zeger & Liang 1986). The former allows between- and within-patient information to be used equally and the latter adjusts for within-patient correlation thereby discounting between-patient differences. Furthermore, a second set of analyses was undertaken adjusting for categorical drug effects in addition to the measures of adherence. Although the inclusion of such effects would reduce the predictive power of the L_1 and L_2 parameters and the estimated proportion of time with drug concentration below IC_{50} (given that these were specifically derived to take into account between-drug differences), the other parameters examined might be expected to be more predictive when between-drug effects are allowed for.

Only a single adherence measure was included in each model due to the strong correlation between the measures examined. Table 3 demonstrates the significant and strong (in terms of large absolute magnitude) correlations between different adherence measures calculated over the 7 days prior to each clinical measurement. Patient-specific correlations were stronger still.

Data from Kantonsspital St. Gallen, Switzerland were not included in these analyses due to the small number of viral load measurements greater than 400 copies ml^{-1} (less than 2% of measurements). Viral load

data from both Clinical Partners Inc. and trial M99-056 were analysed. However, the models can be fitted only to viral load and $CD4^+$T-cell count data without systematic temporal trends. Therefore, given that M99-056 was a trial of first therapy in previously antiretroviral-naive patients, the first 120 days of viral load data for each patient were excluded from this analysis. This period represents the typical interval over which viral load fell from pre-therapy set point levels to on-therapy residual levels. Moreover, since increases in $CD4^+$T-cell counts following initiation of therapy occur over a much longer time-scale than falls in viral load, it was not possible to incorporate the $CD4^+$T-cell counts from M99-056 in this analysis. Thus, only $CD4^+$T-cell count data from Clinical Partners Inc. were analysed.

Table 4 presents the results from the logistic regression and GEE analyses exploring the correlation between viral load and $CD4^+$T-cell count outcome measures and the short-term adherence measures described above. It is clear that substantial portions of both within- and between-patient variation in outcomes can be explained by adherence to antiretroviral therapy regimens. As expected, the viral-replication-related predictors (namely, pIC_{50}, L_1 and L_2) were strongly predictive of viral load and (except for L_2) $CD4^+$T-cell count. Indeed, when categorical drug effects are not explicitly included in the models, L_1 and L_2 are the best predictors of viral-load. They are superior to the non-pharmacologically based adherence measures although the latter are clearly seen to be predictive of both viral load and $CD4^+$T-cell count outcomes. Associations between the non-pharmacologically based measures and viral load were strengthened when drug effects were included.

These results demonstrate the importance of good adherence in terms of both dose frequency and dose timing in controlling viral load and improving $CD4^+$T-cell counts. The significant correlation obtained (using GEE methods) between adherence and outcome based on within-patient differences underline the potential for patient outcomes to be improved by interventions that lead to improvements in patient adherence. However, the full consequences of past poor adherence may not be fully reversible, if, for example, viral drug resistance had already developed.

It is reassuring to see that summary measures that take into account PK and PD properties of the antiretroviral drugs explain between-patient variation particularly well, despite the fact that other key determinants of between-patient variation in both viral load and CD4 counts are not accounted for. Thus, further analyses of larger patient populations using these methods, when such data become available, could estimate the proportion of variation in outcomes between patient subgroups that is due to systematic differences in adherence practices.

7. DISCUSSION

Understanding determinants of clinical outcome for antiretroviral therapy in HIV infection is fundamental to improving the long-term sustainability of treatment. The difference between treatment success levels seen in controlled clinical trials and those in observational studies can be marked, and adherence is often suggested as a potential cause (Deeks *et al.* 1997; Staszewski *et al.* 1999; Matthews *et al.* 2002). Indeed, it is a truism that patient adherence is critical to treatment success—a drug needs to be taken to have an effect. However, quantifying the impact of adherence on the real-world efficacy of antiretroviral regimens is far from straightforward. It requires real-world patterns of adherence behaviour to be characterized, and the relationship between particular patterns of adherence and clinical outcomes to be quantified. This paper approaches these challenges in three ways: visualizing adherence patterns captured by electronic monitoring of pill bottle openings; using simple models to describe individual patterns of adherence and between-patient variability; and developing new viral-replication-related measures incorporating PK/PD to predict HIV treatment outcome.

The variety of visualization approaches introduced in figure 1 highlights a key aspect of observed adherence behaviour: that dose frequency adherence (taking a certain number of pills per day) is only a part of overall adherence behaviour. Timing adherence—the extent to which a patient takes drug doses at the prescribed times, and the level of random and systematic deviation from optimal (namely identical) inter-dose intervals—is also crucial.

The simple model of dose timing introduced in this paper nicely distinguishes these two aspects of adherence behaviour (figures 4 and 5). It illustrates a key observation—that a high level of dose frequency adherence is not necessarily predictive of good adherence to dose timing. Hence, both aspects of 'good' adherence behaviour may need to be given greater emphasis in patient follow-up. The adherence model developed is parameterized in terms of simple summary statistics of frequency and timing adherence. The distribution of estimated values of these parameters provides insight into population variation in adherence behaviour.

Further work is required to extend the adherence model to capture longer time-scale changes in adherence patterns, whether the result of long-term continuous changes in behaviour, or discontinuities caused by regimen changes or drug holidays. However, the model presented here is sufficiently simple to be readily embedded within more sophisticated frameworks.

In relating adherence behaviour to clinical outcome, two strategies are available: developing a predictive mathematical model of HIV replication incorporating realistic PK/PD, or developing statistical (regression) models capturing the observed correlation between clinical outcome and adherence measures. The first approach is mechanistic (in the sense of capturing biological processes underlying clinical outcome), while the second is purely descriptive. Mathematical modelling of HIV has been the topic of much past work (Perelson *et al.* 1996, 1997; Bonhoeffer *et al.* 1997; Ferguson *et al.* 1999; Phillips *et al.* 2001); however, these models have rarely incorporated realistic PK/PD or adherence behaviour (Wahl & Nowak 2000;

Table 4. Logistic regression results.

(Significant results are presented in boldface type (and italicized for the log odds ratio) for emphasis. The predictors, except for L_2, were calculated over various time-intervals (3, 5, 7, 14, 21, 28 and 35 days) prior to the clinical measurement.)

		days before clinical measurement					
		3	7	14	21	28	35
(*a*) *analysis of the binary variable (viral load≤400 copies ml^{-1}) without categorical drug effects*							
p	log odds ratio	0.142	*1.163*	*1.253*	1.176	*1.379*	*1.420*
	p-value	0.807	**0.025**	**0.027**	0.057	**0.029**	**0.031**
	GEE *p*-value	0.874	0.064	**0.030**	0.061	**0.029**	**0.030**
s.d.	log odds ratio	−0.026	−0.011	−0.013	*−0.032*	*−0.025*	−0.011
	p-value	0.554	0.707	0.088	**0.004**	**0.015**	0.159
	GEE *p*-value	0.553	0.689	0.137	**0.031**	**0.005**	0.160
var	log odds ratio	-1.400×10^{-4}	5.280×10^{-4}	-8.060×10^{-5}	-3.542×10^{-4}	-1.656×10^{-4}	-1.989×10^{-5}
	p-value	0.955	0.703	0.177	**0.027**	0.205	0.750
	GEE *p*-value	0.944	0.546	0.187	0.124	**0.030**	0.587
pIC_{50}	log odds ratio	*−2.127*	*−2.243*	*−2.006*	*−2.381*	−2.391	*−1.702*
	p-value	**0.014**	**0.004**	**0.008**	**0.003**	**0.004**	**0.050**
	GEE *p*-value	0.079	**0.031**	**0.018**	**0.007**	**0.005**	**0.029**
L_1	log odds ratio	*−0.084*	*−0.032*	*−0.014*	*−0.010*	*−0.007*	*−0.005*
	p-value	**<0.001**	**<0.001**	**<0.001**	**<0.001**	**<0.001**	**<0.001**
	GEE *p*-value	**<0.001**	**<0.001**	**<0.001**	**<0.001**	**<0.001**	**<0.001**
L_2	log odds ratio	*−0.189*					
	p-value	**<0.001**					
	GEE *p*-value	**<0.001**					
(*b*) *analysis of the binary variable (viral load≤400 copies ml^{-1}) with categorical drug effects*							
p	log odds ratio	1.101	*1.817*	*1.552*	*1.311*	*1.528*	*1.517*
	p-value	0.078	**0.002**	**0.018**	0.075	**0.040**	0.053
	GEE *p*-value	0.206	0.022	0.055	**<0.001**	**<0.001**	**<0.001**
s.d.	log odds ratio	0.026	−0.002	*−0.021*	*−0.040*	*−0.036*	*−0.019*
	p-value	0.640	0.951	**0.010**	**0.002**	**0.002**	**0.028**
	GEE *p*-value	0.610	0.949	**0.042**	**<0.001**	**<0.001**	**<0.001**
var	log odds ratio	1.243×10^{-3}	5.486×10^{-4}	-1.288×10^{-4}	-4.475×10^{-4}	-2.624×10^{-4}	-5.387×10^{-5}
	p-value	0.698	0.634	**0.040**	**0.009**	0.056	0.360
	GEE *p*-value	0.583	0.409	0.073	**<0.001**	**<0.001**	**<0.001**
pIC_{50}	log odds ratio	−0.667	−1.085	−1.481	*−1.291*	*−1.477*	*−0.929*
	p-value	0.540	0.263	0.113	0.202	0.158	0.413
	GEE *p*-value	0.654	0.376	0.211	**<0.001**	**<0.001**	**<0.001**
L_1	log odds ratio	0.004	−0.008	−0.005	−0.004	−0.002	−0.001
	p-value	0.878	0.355	0.124	0.143	0.337	0.586
	GEE *p*-value	0.898	0.469	0.261	0.247	0.411	0.654
L_2	log odds ratio	*−0.129*					
	p-value	**0.005**					
	GEE *p*-value	**0.027**					
(*c*) *analysis of the binary variable (CD4$^+$ T-cell count≤600 cells mm^{-3}) without categorical drug effects*							
p	log odds ratio	−1.437	*−3.322*	*−5.037*	*−5.858*	*−6.135*	*−5.491*
	p-value	0.150	**0.033**	**0.018**	**0.017**	**0.016**	**0.029**
	GEE *p*-value	0.067	**0.024**	**0.030**	**0.014**	**0.016**	**0.011**
s.d.	log odds ratio	0.056	0.106	0.119	*0.146*	*0.188*	*0.170*
	p-value	0.373	0.134	0.107	0.059	**0.031**	**0.049**
	GEE *p*-value	0.398	0.143	0.128	**0.038**	**0.025**	**0.013**
var	log odds ratio	0.002	0.009	*0.011*	*0.014*	*0.019*	*0.018*
	p-value	0.562	0.228	0.163	0.139	0.097	0.108
	GEE *p*-value	0.521	0.213	**<0.001**	**<0.001**	**<0.001**	**0.022**
pIC_{50}	log odds ratio	2.354	*3.124*	2.952	*3.737*	*3.817*	*3.950*
	p-value	0.097	**0.040**	0.062	**0.031**	**0.029**	**0.040**
	GEE *p*-value	0.173	**0.049**	0.066	**0.037**	**0.029**	**0.027**
L_1	log odds ratio	*0.051*	*0.022*	*0.009*	*0.006*	*0.005*	*0.004*
	p-value	**0.025**	**0.011**	**0.036**	**0.019**	**0.022**	**0.034**
	GEE *p*-value	0.082	**0.032**	0.066	**0.037**	**0.043**	0.053
L_2	log odds ratio	0.032					
	p-value	0.552					
	GEE *p*-value	0.642					

(*Continued.*)

Table 4. (*Continued.*)

		days before clinical measurement					
		3	7	14	21	28	35
(*d*) *analysis of the binary variable (CD4$^+$ T-cell count* $\leq$ *600 cells mm^{-3}) with categorical drug effects*							
p	log odds ratio	−1.449	*−3.271*	*−5.059*	*−5.760*	*−6.058*	*−5.633*
	p-value	0.157	**0.034**	**0.018**	**0.019**	**0.019**	**0.028**
	GEE *p*-value	0.076	**0.024**	**0.032**	**0.017**	**0.017**	**0.010**
s.d.	log odds ratio	0.057	0.106	0.124	*0.156*	*0.194*	*0.184*
	p-value	0.358	0.131	0.091	**0.049**	**0.029**	**0.043**
	GEE *p*-value	0.370	0.137	0.114	**0.036**	**0.022**	**0.013**
var	log odds ratio	0.002	0.009	*0.012*	*0.016*	*0.020*	*0.019*
	p-value	0.542	0.219	0.139	0.112	0.085	0.096
	GEE *p*-value	0.507	0.210	**<0.001**	**<0.001**	**<0.001**	**0.026**
pIC_{50}	log odds ratio	2.269	*3.036*	2.910	*3.604*	*3.584*	*3.818*
	p-value	0.111	**0.046**	0.067	**0.039**	**0.041**	**0.050**
	GEE *p*-value	0.191	**0.046**	0.054	**0.034**	**0.033**	**0.029**
L_1	log odds ratio	0.044	*0.019*	0.007	0.006	0.004	0.003
	p-value	0.082	**0.042**	0.101	0.056	0.066	0.092
	GEE *p*-value	0.239	0.099	0.141	0.103	0.121	0.140
L_2	log odds ratio	0.025					
	p-value	0.631					
	GEE *p*-value	0.702					

Ferguson 2002). Existing models remain, at best, exploratory rather than predictive. They highlight the complex and nonlinear relationship predicted between adherence and clinical outcome. However, these models have not yet successfully been applied to predict the outcome of a clinical trial, for instance. Purely statistical approaches (Vanhove *et al.* 1996; Bangsberg *et al.* 2001; Gross *et al.* 2001; Alexander *et al.* 2003) have been used to demonstrate a strong correlation between simple adherence statistics (e.g. proportion of doses taken) and clinical outcome. However, such models are at best weakly predictive and not easily generalized—for example, in predicting differences between antiretroviral regimens in the dependence of clinical outcome on adherence levels.

It is for these reasons that we have developed an intermediate approach by constructing a simple mathematical model of the relationship between adherence, drug levels and viral replication. This model could be solved analytically to provide a means of transforming a time-series of pill bottle opening events into predicted rates of viral replication over time. Despite the relative simplicity of the model (e.g. only the PI component of regimens is modelled, target cell dynamics are not included, etc.), we have shown that the resulting adherence statistics are better predictors of viral load than a wide range of adherence measures that do not incorporate PK/PD, when categorical drug effects have not been included. Particularly encouraging is the ability of these new measures to explain between-patient differences in the relationship between adherence and clinical outcome.

Future work will explore how the existing framework can be extended to model multiple drugs simultaneously, with the aim of increasing the model's predictive ability. With more data than were available for the current study, the methods presented here offer the potential to distinguish differences between antiretroviral regimens in how sensitive clinical outcomes are to suboptimal adherence. Another focus will be developing the model to predict transitions in viral load or CD4$^+$T-cell count, rather than just levels. This is necessary because adherence thresholds associated with initial suppression of viral load to below the assay LOQ, maintenance of low viral load and viral load rebound may be very different. Thus, a model focused on predicting multiple transition types may have improved predictive ability, albeit at the cost of increased numbers of parameters.

We thank Abbott Laboratories for research funding. N.M.F. also thanks The Royal Society and J.H. thanks the Medical Research Council for fellowship and studentship funding. We thank David Cox for advice on adherence modelling. N.M.F., C.A.D., A.C.G., C.F. and R.M.A. have previously acted as paid consultants to Abbott Laboratories.

REFERENCES

Abbott 1999 *Norvir (ritonavir capsules) soft gelatin (ritonavir oral solution).* Abbott Park, IL: Abbott Laboratories.

Abbott 2001 *Kaletra (lopinavir/ritonavir) prescribing information* Abbott Park, IL: Abbott Laboratories.

Adkins, J. C. & Faulds, D. 1998 Amprenavir. *Drugs* **55**, 837–842.

Alexander, C. S., Asselin, J. J., Ting, L. S., Montaner, J. S., Hogg, R. S., Yip, B., O'Shaughnessy, M. V. & Harrigan, P. R. 2003 Antiretroviral concentrations in untimed plasma samples predict therapy outcome in a population with advanced disease. *J. Infect. Dis.* **188**, 541–548.

Bangsberg, D. R., Hecht, F. M., Charlebois, E. D., Zolopa, A. R., Holodniy, M., Sheiner, L., Bamberger, J. D., Chesney, M. A. & Moss, A. 2000 Adherence to protease inhibitors, HIV-1 viral load, and development of drug resistance in an indigent population. *AIDS* **14**, 357–366.

Bangsberg, D. R., Perry, S., Charlebois, E. D., Clark, R. A., Roberston, M., Zolopa, A. R. & Moss, A. 2001 Non-adherence to highly active antiretroviral therapy predicts progression to AIDS. *AIDS* **15**, 1181–1183.

Barry, M., Gibbons, S., Back, D. & Mulcahy, F. 1997 Protease inhibitors in patients with HIV disease. *Clin. Pharmacokinet.* **32**, 194–209.

Bonhoeffer, S., May, R. M., Shaw, G. M. & Nowak, M. A. 1997 Virus dynamics and drug therapy. *Proc. Natl Acad. Sci. USA* **94**, 6971–6976.

Buss, N., Snell, P., Bock, J., Hsu, A. & Jorga, K. 2001 Saquinavir and ritonavir pharmacokinetics following combined ritonavir and saquinavir (soft gelatin capsules) administration. *Br. J. Clin. Pharmacol.* **52**, 255–264.

De Boer, R. J. & Perelson, A. S. 1998 Target cell limited and immune control models of HIV infection: a comparison. *J. Theor. Biol.* **190**, 201–214.

Deeks, S. G., Smith, M., Holodniy, M. & Kahn, J. O. 1997 HIV-1 protease inhibitors—a review for clinicians. *J. Am. Med. Assoc.* **277**, 145–153.

Eron, J. J. *et al.* 2004 Once-daily vs. twice-daily lopinavir/ritonavir in antiretroviral-naive HIV-positive patients: a 48-week randomized clinical trial. *J. Infect. Dis.* **189**, 265–272.

Ferguson, N. M. 2002 Why do people fail therapy? Modelling adherence and residual replication. In *Overcoming resistance* (ed. J. Weber), pp. 12–17. London: Mediscript.

Ferguson, N. M. *et al.* 1999 Antigen-driven CD4+T cell and HIV-1 dynamics: residual viral replication under highly active antiretroviral therapy. *Proc. Natl Acad. Sci. USA* **96**, 15 167–15 172.

Ferguson, N. M., Fraser, C. & Anderson, R. M. 2001 Viral dynamics and anti-viral pharmacodynamics: rethinking in vitro measures of drug potency. *Trends Pharmacol. Sci.* **22**, 97–100.

Fraser, C., Ferguson, N. M. & Anderson, R. M. 2001 Quantification of intrinsic residual viral replication in treated HIV-infected patients. *Proc. Natl Acad. Sci. USA* **98**, 15 167–15 172.

Frost, S. D. W., Martinez-Picado, J., Ruiz, L., Clotet, B. & Brown, A. J. L. 2002 Viral dynamics during structured treatment interruptions of chronic human immunodeficiency virus type 1 infection. *J. Virol.* **76**, 968–979.

Frottier, J., Meynard, J. L., Morand-Joubert, L. & Guiguet, M. 1998 Factors predictive of early virologic response after a first treatment with a protease inhibitor in the course of HIV infection. *Bull. Acad. Natl Med.* **182**, 981–992. (discussion 992–995).

Girard, P., Blaschke, T. F., Kastrissios, H. & Sheiner, L. B. 1998 A Markov mixed effect regression model for drug compliance. *Stat. Med.* **17**, 2313–2333.

GlaxoSmithKline 2002 *Agenerase (amprenavir) capsules.* Research Triangle Park, NC: GlaxoSmithKline.

Gross, R., Bilker, W. B., Friedman, H. M. & Strom, B. L. 2001 Effect of adherence to newly initiated antiretroviral therapy on plasma viral load. *AIDS* **15**, 2109–2117.

Ho, D. D., Neumann, A. U., Perelson, A. S., Chen, W., Leonard, J. M. & Markowitz, M. 1995 Rapid turnover of plasma virions and CD4 lymphocytes in HIV-1 infection. *Nature* **373**, 123–126.

Hooper, J. 2002 Adherence, resistance and clinical response during antiretroviral therapy. Department of Zoology. University of Oxford.

Hsu, A. *et al.* 1998 Pharmacokinetic interaction between ritonavir and indinavir in healthy volunteers. *Antimicrob. Agents Chemother.* **42**, 2784–2791.

Jarvis, B. & Faulds, D. 1998 Nelfinavir: a review of its therapeutic efficacy in HIV infection. *Drugs* **56**, 147–167.

Kastrissios, H., Suarez, J. R., Katzenstein, D., Girard, P., Sheiner, L. B. & Blaschke, T. F. 1998 Characterizing patterns of drug-taking behavior with a multiple drug regimen in an AIDS clinical trial. *AIDS* **12**, 2295–2303.

Kempf, D. J. *et al.* 1997 Pharmacokinetic enhancement of inhibitors of the human immunodeficiency virus protease by coadministration with ritonavir. *Antimicrob. Agents Chemother.* **41**, 654–660.

Knobel, H., Guelar, A., Carmona, A., Espona, M., Gonzalez, A., Lopez-Colomes, J. L., Saballs, P., Gimeno, J. L. & Diez, A. 2001 Virologic outcome and predictors of virologic failure of highly active antiretroviral therapy containing protease inhibitors. *AIDS Patient Care STDs* **15**, 193–199.

Kurowski, M., Kaeser, B., Sawyer, A., Popescu, M. & Mrozikiewicz, A. 2002 Low-dose ritonavir moderately enhances nelfinavir exposure. *Clin. Pharmacol. Theor.* **72**, 123–132.

Liang, K. Y. & Zeger, S. L. 1986 Longitudinal data-analysis using generalized linear-models. *Biometrika* **73**, 13–22.

Little, S. J., McLean, A. R., Spina, C. A., Richman, D. D. & Havlir, D. V. 1999 Viral dynamics of acute HIV-1 infection. *J. Exp. Med.* **190**, 841–850.

Masquelier, B. *et al.* 2002 Mechanisms of early virologic failure in antiretroviral-naive patients starting protease inhibitor-containing regimens: the APROVIR study. *J. Infect. Dis.* **186**, 1503–1507.

Matthews, G. V., Sabin, C. A., Mandalia, S., Lampe, F., Phillips, A. N., Nelson, M. R., Bower, M., Johnson, M. A. & Gazzard, B. 2002 Virological suppression at 6 months is related to choice of initial regimen in antiretroviral-naive patients: a cohort study. *AIDS* **16**, 53–61.

McNabb, J. J., Nicolau, D. P., Stoner, J. A. & Ross, J. 2003 Patterns of adherence to antiretroviral medications: the value of electronic monitoring. *AIDS* **17**, 1763–1767.

Melbourne, K. M., Geletko, S. M., Brown, S. L., Willey-Lessne, C., Chase, S. & Fisher, A. 1999 Medication adherence in patients with HIV infection: a comparison of two measurement methods. *AIDS Read.* **9**, 329–338.

Merck & Co., Inc. 1999 *Crixivan (indinavir sulfate) capsules.*

Miller, L. G. & Hays, R. D. 2000 Measuring adherence to antiretroviral medications in clinical trials. *HIV Clin. Trials* **1**, 36–46.

Molla, A. *et al.* 1998 Human serum attenuates the activity of protease inhibitors toward wild-type and mutant human immunodeficiency virus. *Virology* **250**, 255–262.

Montaner, J. S., Hogg, R., Raboud, J., Harrigan, R. & O'Shaughnessy, M. 1998 Antiretroviral treatment in 1998. *Lancet* **352**, 1919–1922.

Perelson, A. S., Neumann, A. U., Markowitz, M., Leonard, J. M. & Ho, D. D. 1996 HIV-1 dynamics *in vivo*: virion clearance rate, infected cell life-span and viral generation time. *Science* **271**, 1582–1586.

Perelson, A. S., Essunger, P., Cao, Y., Vesanen, M., Hurley, A., Saksela, K., Markowitz, M. & Ho, D. D. 1997 Decay characteristics of HIV-1-infected compartments during combination therapy. *Nature* **387**, 188–191.

Phillips, A. N., Youle, M., Johnson, M. & Loveday, C. 2001 Use of a stochastic model to develop understanding of the impact of different patterns of antiretroviral drug use on resistance development. *AIDS* **15**, 2211–2220.

Roche 1997 *Fortovase (saquinavir).* (1997). Nutley, NJ: Roche Laboratories, Inc.

Staszewski, S., Miller, V., Sabin, C. A., Carlebach, A., Berger, A. M., Weidmann, E., Helm, E. B., Hill, A. & Phillips, A. N. 1999 Virological response to protease inhibitor therapy in an HIV clinic cohort. *AIDS* **13**, 367–373.

van Heeswijk, R. P. G., Veldkamp, A. I., Hoetelmans, R. M. W., Mulder, J. W., Schreij, G., Hsu, A., Lange, J. M. A., Beijnen, J. H. & Meenhorst, P. L. 1999 The steady-state plasma pharmacokinetics of indinavir alone and in combination with a low dose of ritonavir in twice daily dosing regimens in HIV-1-infected individuals. *AIDS* **13**, F95–F99.

Vanhove, G. F., Schapiro, J. M., Winters, M. A., Merigan, T. C. & Blaschke, T. F. 1996 Patient compliance and drug failure in protease inhibitor monotherapy. *J. Am. Med. Assoc.* **276**, 1955–1956.

Wahl, L. M. & Nowak, M. A. 2000 Adherence and drug resistance: predictions for therapy outcome. *Proc. R. Soc. B* **267**, 835–843. (doi:10.1098/rspb.2000.1079.)

Wong, D., Modi, R. & Ramanathan, M. 2003 Assessment of Markov-dependent stochastic models for drug administration compliance. *Clin. Pharmacokinet.* **42**, 193–204.

Zeger, S. L. & Liang, K. Y. 1986 Longitudinal data analysis for discrete and continuous outcomes. *Biometrics* **42**, 121–130.